6-17-2013

Enhanced, Fast-running Scaling Law Model of Thermal Blooming and Turbulence Effects on High Energy Laser Propagation

Noah R. Van Zandt

Steven T. Fiorino
Air Force Institute of Technology

Kevin J. Keefer
Air Force Institute of Technology

Recommended Citation

Noah R. Van Zandt, Steven T. Fiorino, and Kevin J. Keefer, "Enhanced, fast-running scaling law model of thermal blooming and turbulence effects on high energy laser propagation," Opt. Express 21, 14789-14798 (2013). https://doi.org/10.1364/OE.21.014789

Enhanced, fast-running scaling law model of thermal blooming and turbulence effects on high energy laser propagation

Noah R. Van Zandt, Steven T. Fiorino,* and Kevin J. Keefer

Department of Engineering Physics – Center for Directed Energy, Air Force Institute of Technology, 2950 Hobson Way, Wright-Patterson AFB, OH 45433-7756, USA

Steven.Fiorino@afit.edu

Abstract: A new scaling law model is presented to rapidly simulate thermal blooming and turbulence effects on high energy laser propagation, producing results approaching the quality normally only available using wave-optics code, but at much faster speed. The model convolves irradiance patterns originating from two distinct scaling law models, one with a proficiency in thermal blooming effects and the other in turbulence. To underscore the power of the new model, results are verified for typical, realistic scenarios by direct comparison with wave optics simulation.

OCIS codes: (010.0010) Atmospheric and oceanic optics; (010.1300) Atmospheric propagation; (010.1330) Atmospheric turbulence; (010.7060) Turbulence.

References and links

1. H. T. Yura, "Atmospheric turbulence induced laser beam spread," Appl. Opt. **10**(12), 2771–2773 (1971).
2. H. Breaux, W. Evers, R. Sepucha, and C. Whitney, "Algebraic model for cw thermal-blooming effects," Appl. Opt. **18**(15), 2638–2644 (1979).
3. F. G. Gebhardt, "Twenty-five years of thermal blooming: an overview," Proc. SPIE **1221**, 2–25 (1990).
4. R. J. Bartell, G. P. Perram, S. T. Fiorino, S. N. Long, M. J. Houleb, C. A. Rice, Z. P. Manning, D. W. Bunch, M. J. Krizo, and L. E. Gravley, "Methodology for comparing worldwide performance of diverse weight-constrained high energy laser systems," Proc. SPIE **5792**, 76–87 (2005).
5. N. R. Van Zandt, S. J. Cusumano, R. J. Bartell, S. Basu, J. E. McCrae, and S. T. Fiorino, "Comparison of coherent and incoherent laser beam combination for tactical engagements," Opt. Eng. **51**(10), 104301 (2012).
6. A. M. Ngwele and M. R. Whiteley, "Scaling Law Modeling of Thermal Blooming in Wave Optics," MZA Associates Corporation, Dayton, Technical Report NGIT ABL A&AS, 2006.
7. S. T. Fiorino, R. M. Randall, M. F. Via, and J. L. Burley, "Validation of a UV to RF high spectral resolution atmospheric boundary layer characterization tool," J. Appl. Meteorol. Climatol. (in review).
8. S. T. Fiorino, R. M. Randall, R. J. Bartell, A. D. Downs, P. C. Chu, and C. W. Fan, "Climate change: anticipated effects on high-energy laser weapon systems in maritime environments," J. Appl. Meteorol. Climatol. **50**(1), 153–166 (2011).
9. C. L. Leakeas, R. J. Bartell, M. J. Krizo, S. T. Fiorino, S. J. Cusumano, and M. R. Whiteley, "Effects of thermal blooming on systems comprised of tiled subapertures," Proc. SPIE **7685**, 267–269 (2010).
10. M. R. Whiteley, E. P. Magee, and A. M. Ngwele, "Scaling for High Energy Laser and Relay Engagement (SHaRE) User Guide," MZA Associates, Dayton OH, (2011).
11. M. R. Whiteley, "Thermal Blooming Modeling in SHaRE," presented at the DoD High Energy Laser Joint Technology Office Workshop, Air Force Institute of Technology, WPAFB, OH, 9–10 Oct. 2008.
12. S. C. Coy and B. P. Venet, "WaveTrain™ User Guide" (MZA Associates Corporation, Copyright © 1995 – 2010), http://www.mza.com/doc/wavetrain/wtug/index.htm.
13. SAIC Final Report, "Analytic Model for Adaptive Optical Compensation of Thermal Blooming (AOTB)," Govt Contract #FA9451–10-D-0250, (2012).
14. J. D. Barchers, "Linear analysis of thermal blooming compensation instabilities in laser propagation," J. Opt. Soc. Am. A **26**(7), 1638–1653 (2009).
15. R. A. Motes, S. A. Shakir, and R. W. Berdine, "An efficient scalar, non-paraxial beam propagation method," J. Lightwave Technol. **30**(1), 4–8 (2012).
16. B. G. Ward, "Modeling of transient modal instability in fiber amplifiers," Opt. Express **21**(10), 12053–12067 (2013).
17. S. T. Fiorino, R. M. Randall, F. J. Echeverria, R. J. Bartell, M. J. Krizo, and S. J. Cusumano, "Effectiveness assessment of tactical laser engagement scenarios in the lower atmosphere," J. Aero. Inf. Sys. **10**(1), 32–38 (2013).

#188462 - $15.00 USD Received 8 Apr 2013; revised 1 Jun 2013; accepted 3 Jun 2013; published 13 Jun 2013

1. Introduction

The Directed Energy (DE) community has come to rely on fast-running scaling law codes to efficiently model high energy laser (HEL) propagation and beam control performance and to provide a first-order, broad-ranging assessment of a laser system and its concept of employment [1–4]. Furthermore, simulations using scaling laws are computationally fast enough to allow the inclusion of complex, but physically realistic, environmental effects which are often not part of wave optics studies. Thus, HEL scaling law codes are well-suited for size, weight, and power optimization or input to simulations of force-on-force engagements. Nevertheless, though often anchored in rigorous, first-principles wave optics code, scaling law algorithms have yet to exhibit the fidelity of the former, especially when simulating non-linear propagation effects such as those that arise through the interaction of thermal blooming and optical turbulence. Additionally, simple thermal blooming metrics such as distortion number and critical power have not shown direct correlation with wave optics irradiance patterns [5,6]. For these reasons and to enhance their utility, we explored the possibility of convolving the far-field irradiance patterns from optimized scaling-law models—each delivering outcomes comparable to wave optics simulation in certain regimes—retaining the advantage of speed while providing higher quality laser performance simulation.

In this paper we describe our new, fast-calculating HEL scaling law model and its ability to capture the shape and displacement of a thermally-bloomed far-field irradiance pattern in the presence of turbulence. To verify improvements, we compare parametrics such as far-field irradiance and its centroid tilt produced by the new model with those parameters derived through implementation of traditional wave optics code for scenarios conducive to optical turbulence and thermal blooming effects. Further strengthening our conclusions, we applied the model to multiple scenarios, simulating both horizontal and oblique realistic engagement geometries.

2. Approach: update existing end-to-end scaling law simulation using convolution

The new HEL scaling law model described herein benefits from its simplicity and strengths of constituent parts. We convolve the far-field irradiance pattern calculated by the High Energy Laser End to End Operational Simulation (HELEEOS) with that of the recently released Adaptive Optical Compensation of Thermal Blooming (AOTB) model. HELEEOS, developed by the United States Air Force Institute of Technology (AFIT), is the beneficiary of AFIT's Laser Environmental Effects Definition and Reference (LEEDR) model [7]. As such, HELEEOS is the first end-to-end directed energy propagation model to incorporate probabilistic, climatological data so as to develop temporally and spatially variable meteorological, aerosol, and turbulence profiles and in turn enable realistic evaluation of laser propagation, imaging, and adaptive-optics systems [8,9]. HELEEOS also uses an embedded toolbox, Scaling for High Energy Laser and Relay Engagement (SHARE), developed by MZA Associates [10]. The SHARE toolbox supports HELEEOS' beam metrics and irradiance calculations through scaling law treatments of propagation and atmospheric beam control anchored and optimized through extensive empirical analysis using wave optics simulations. Though HELEEOS, via SHARE scaling laws, is capable of producing far-field irradiance patterns indicative of both optical turbulence and thermal blooming effects [11], comparison with standard wave optics output suggests strongest correlation when one selects HELEEOS to calculate only the turbulence effect. The simplified Gaussian form, g, of HELEEOS' embedded SHARE scaling law for turbulence effects on the far-field irradiance is

$$g(x,y) = E_{peak} \exp\left[-0.5\left(x^2/\sigma_x^2 + y^2/\sigma_y^2\right)\right] \quad (1)$$

where E_{peak} is the peak irradiance, x and y are the spatial dimensions, and σ_x and σ_y are the beam widths in their respective dimensions. When turbulence is the only distortion effect, σ_x and σ_y are equal in Eq. (1). Figure 1 compares a HELEEOS far-field irradiance pattern with that of the analytic output of wave optics code for a typical near-surface, oblique path laser

#188462 - $15.00 USD Received 8 Apr 2013; revised 1 Jun 2013; accepted 3 Jun 2013; published 13 Jun 2013

engagement capturing optical turbulence, but excluding thermal blooming effects. For reference, we used MZA Associates' WaveTrain™ for our wave optics simulations presented throughout this paper [12]. The comparison is quite good by scaling law standards, albeit the HELEEOS pattern is perfectly gaussian, while that from wave optics is a bit more complex, showing irradiance beyond the $1/e^2$ point and slight inhomogeneities inherent in its Monte Carlo analysis.

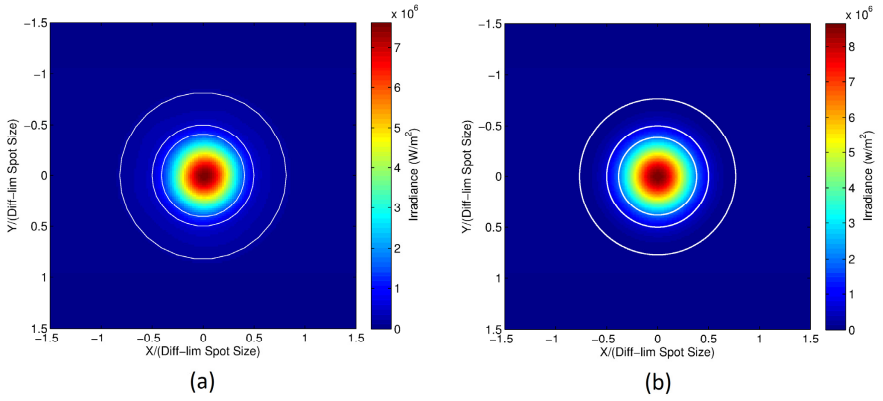

Fig. 1. Wave optics (a) and HELEEOS (b) far-field irradiance patterns for a 7.5 km slant path, air to surface engagement exclusive of thermal blooming effects. The center- to outer-most calibration rings about the central propagation axis in this and subsequent figures have arbitrarily sized diameters to represent the diffraction-limit, 5-cm and 10-cm, respectively. Note: HELEEOS' Gaussian scaling law approximation matches wave optics very well.

As its name implies, the AOTB model is an outgrowth of recent research tied to analytical evaluation of the stability of optical turbulence compensation in the presence of thermal blooming [13]. Like HELEEOS, this new scaling law model is also a fast-running semi-analytical code, but does not rely on empirically-derived solutions or lookup tables derived from wave optics calculations. Rather, AOTB was developed solely from first-principles. Using the Rytov approximation to linearize the thermal blooming compensation equations [14], an AOTB strength lies in its speedy calculation of whole-beam thermal blooming merged with turbulence-induced fine-scale blooming effects in an effort to properly evaluate instabilities otherwise due to one's compensation for such turbulence. With this objective in mind, the whole-beam thermal blooming solution is a direct output of the currently configured simulation, whereas "blurring" of such output due to interaction with turbulence has been reserved to future work. Nonetheless, Fig. 2 captures the superior correlation of the AOTB and wave optics codes' whole-beam thermal blooming far-field patterns for our near-surface, oblique laser engagement. Of interest, both codes produce an irradiance pattern with a classic crescent-shape and displacement into the cooler, effective cross-beam airflow. Each was initialized with a realistic, LEEDR-generated atmosphere, which as we noted earlier, is also typically done when executing HELEEOS. Also note AOTB and the wave optics simulations were run with a zero random wind component along the path to give deterministic results. This approach avoids Monte Carlo analysis while remaining statistically identical to the more realistic case of a non-zero random wind component when stagnation zones are not present, as is always the case in this work.

#188462 - $15.00 USD Received 8 Apr 2013; revised 1 Jun 2013; accepted 3 Jun 2013; published 13 Jun 2013

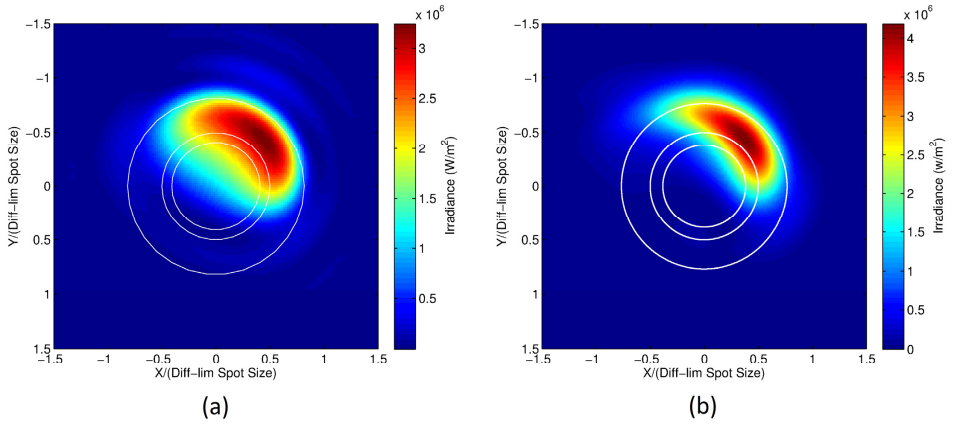

Fig. 2. A comparison of wave optics (a) and AOTB (b) far-field irradiance patterns for the 7.5 km slant path, air-to-surface engagement. Since the two methods model thermal blooming differently, the minor differences in the irradiance patterns are expected.

Given each model's current status of evolution and verification with wave-optics simulations (HELEEOS specializing in representative far-field irradiance patterns due to turbulence and AOTB configured to output advanced whole-beam thermal blooming solutions), we decided to convolve their respective irradiance patterns and compare with a wave-optics simulation of both thermal blooming and turbulence. By making use of the well-known convolution theorem in Eq. (2) below, this operation can be performed in Fourier space, reducing computation time to an insignificant fraction of a second when run on a modern personal computer.

$$\mathcal{F}\{g(x,y)\otimes h(x,y)\}=\mathcal{F}\{g(x,y)\}\mathcal{F}\{h(x,y)\} \tag{2}$$

where g represents the turbulence blurred irradiance pattern (other blurring effects can also be included here) from HELEEOS and h the thermally bloomed irradiance pattern from AOTB. The output of the convolution is then given by

$$\begin{aligned} g(x,y)\otimes h(x,y) = 2\pi E_{peak}\sigma_x\sigma_y \iint \exp\left[-2\pi^2\left(\sigma_x^2 f_x^2+\sigma_y^2 f_y^2\right)\right] \\ \times\mathcal{F}\{h(x,y)\}\exp\left[j2\pi\left(f_x x+f_y y\right)\right]df_x df_y \end{aligned} \tag{3}$$

When we convolved HELEEOS turbulence-only [Fig. 1(b)] and AOTB thermal blooming-only [Fig. 2(b)] irradiance patterns, it yielded a result [Fig. 3(b)] which correlates quite well with the output from first-principles wave optics simulation [Fig. 3(a)] of both thermal blooming and turbulence. Prior to development and implementation of this convolution step inside the HELEEOS update (hereafter referred to as HELEEOS – AOTB), legacy HELEEOS calculations for scenarios of thermal blooming and turbulence produced outcomes shown in Fig. 3(c). Clearly, HELEEOS – AOTB enables a better solution. The similarities between it and wave optics are dramatic, and the HELEEOS – AOTB output was generated in less than five seconds as compared to over two hours by way of wave-optics code.

#188462 - $15.00 USD Received 8 Apr 2013; revised 1 Jun 2013; accepted 3 Jun 2013; published 13 Jun 2013

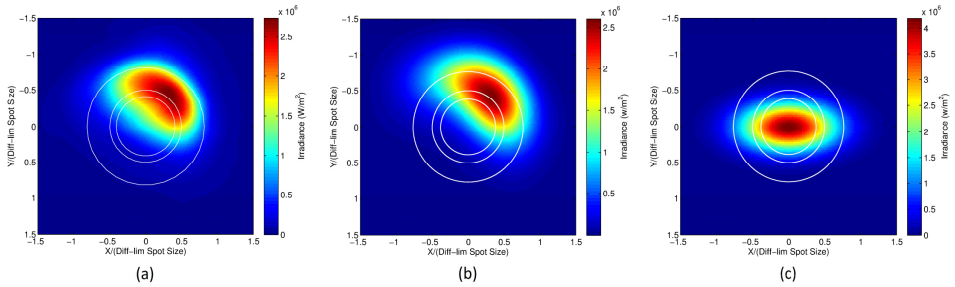

Fig. 3. A comparison of wave optics (a), HELEEOS – AOTB (b), and pre-convolution, legacy HELEEOS (c) far-field patterns for 7.5 km slant path, air to surface laser engagement showing good correlation between HELEEOS – AOTB and wave optics.

Additional run time comparisons are shown in Table 1. With a median reduction of 99.9%, the HELEEOS – AOTB scaling law provides excellent time benefit over wave optics. Of note, our wave optics run times are based on a traditional split-step Fourier propagation approach running on a modern, high-end CPU. In recent years, faster wave optics approaches have been developed, such as Graphics Processing Unit (GPU) implementations and the harmonic-expansion technique [15,16]. These approaches offer about an order of magnitude reduction in run time but are still much slower than HELEEOS – AOTB.

Table 1. Comparison of simulation run times using wave optics and HELEEOS – AOTB for realistic 5 km range scenarios.

Scenario	Turbulence (x HV 5/7)	Wave Optics Run Time[1] (s)	HELEEOS – AOTB Run Time (s)	Reduction[2] (%)
Air to Surface	0	3930	5.0	–99.87%
Air to Surface	1	8500	4.8	–99.94%
Surface to Surface	0	2490	5.2	–99.79%
Surface to Surface	1	34800	5.3	–99.98%

[1]Wave optics run times varied predominately due to changes in grid sizes to preserve accuracy as turbulence increased.
[2]In all cases tested, HELEEOS – AOTB reduced run time by at least 99% with a median reduction of 99.9%.

3. Verification using multiple laser engagement scenarios

To verify fast and representative simulation of complex laser propagation phenomena and applicability to a broad range of realistic engagements, we applied the new HELEEOS – AOTB scaling law model to multiple high-power laser scenarios designed to encounter a variety of thermal blooming and turbulence combinations [5,17]. As such, the platform and target were located within or very close to the atmospheric boundary layer (generally the lowest 1500 m), while propagation paths were defined to be either horizontal or oblique, including surface to surface (S2S), surface to air (S2A), air to surface (A2S), and air to air (A2A). Using LEEDR, all cases implemented realistic atmospheric extinction profiles based on probabilistic climatology for a typical littoral site on a summer afternoon. Our laser was simulated to operate at approximately 1 μm and 60 kW. For a non-water absorbing wavelength, the primary absorption mechanism for inducing heating and thermal blooming is aerosol particulate absorption. We defined wind according to the Bufton profile from the north-east with surface velocity at 5 m/s. Furthermore, the optical turbulence profile for each engagement is scaled according to Hufnagel-Valley 5/7. Scenario specifics are presented in Table 2 below.

As introduced in section 2, we chose to verify the strengths of HELEEOS – AOTB by benchmarking its calculated far-field irradiance pattern at the target relative to similar results obtained with wave-optics code. Prior to introducing these results we think it instructive to

#188462 - $15.00 USD Received 8 Apr 2013; revised 1 Jun 2013; accepted 3 Jun 2013; published 13 Jun 2013

show that the convolution step itself introduces little error. We convolved wave optics solutions for thermal blooming-only [Fig. 4(b)] and turbulence-only [Fig. 4(a)], which produced Fig. 4(c).

Table 2. Scenarios[1] used to verify convolved scaling law model technique.

Scenario	S2S	S2A	A2S	A2A
Platform altitude (m)	15	3	1524	1500
Platform speed (m/s)	0	0	100	100
Platform heading (deg)	0	0	0	45
Target altitude (m)	15	1524	3	1500
Target speed (m/s)	10	100	0	100
Target heading (deg)	90	180	0	180
Turbulence (x HV 5/7)	0.05	1	1	1
Range (m)	5000	5000	7500	10000

[1]Platform / target speeds and headings were selected to produce a variety of thermal blooming and optical turbulence combinations. The target starts due north of the platform.

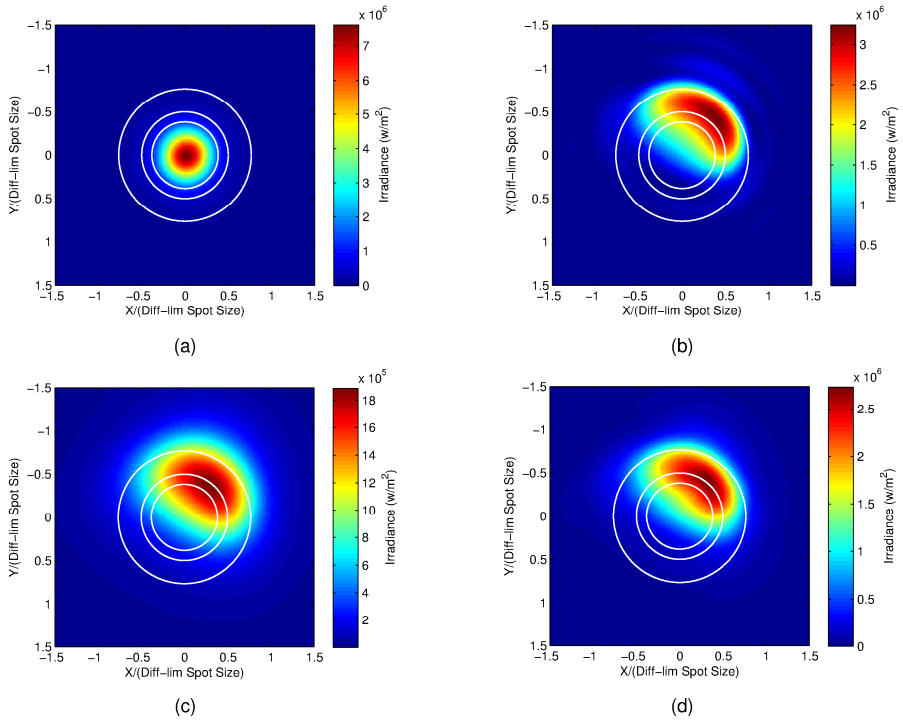

Fig. 4. Wave optics generated far-field irradiance patterns: turbulence-only effects (a); thermal blooming-only effects (b); their convolution (c); and turbulence and thermal blooming effects (d). The comparison of (c) and (d) shows the convolution step is able to reproduce total effects from constituent contributions quite well.

Figure 4(d) represents the wave-optics solution for conditions of thermal blooming and turbulence. A comparison of Figs. 4(c) and 4(d) reveals the very small extent to which convolution itself introduces error. It is worthwhile to note in the limiting case when both aberrations are small and thus both input patterns are nearly Gaussian, the output of convolution will be exactly correct if diffraction effects are included in only one of the inputs, as the convolution of two Gaussians is easily shown to be another Gaussian with squared

#188462 - $15.00 USD Received 8 Apr 2013; revised 1 Jun 2013; accepted 3 Jun 2013; published 13 Jun 2013

beam width equal to the summed squares of the input beam widths: $\sigma^2 = \sigma_1^2 + \sigma_2^2$. Since diffraction effects are present in both inputs (i.e. the irradiance patterns shown in Figs. 4(a) and 4(b)) to the above convolution, the convolved spot shown here indicates additional blurring due to the double counting of diffraction. In practice, this double counting will not be present when scaling law outputs are used as inputs, one of which will artificially neglect diffraction.

Now, we compare the far-field irradiance profiles for our extended set of scenarios presented in Fig. 5 below. In all cases and as anticipated, the far-field irradiance patterns—spots—are bloomed into the effective wind, which blows from varying direction in each geometry due to the relative motion of the platform and target and the natural wind direction. The irradiance profiles generated by HELEEOS – AOTB and those by wave optics compare relatively well in all cases. The spots do not compare perfectly, as all scaling law methods are only an approximation of more detailed treatment of the underlying electro-magnetic and thermodynamic processes, which are more fully captured by wave optics. In general, we also observe HELEEOS – AOTB is a slightly more conservative estimate of performance than wave optics, a characteristic common to many scaling law models.

Having presented our general, qualitative comparison of relative spot size and shape, we move now to a quantitative assessment of relative power-in-the-bucket (PIB), peak irradiance, and centroid tilt. The most common metric for analyzing high-energy laser system performance is PIB, which is simply the power hitting a circular bucket of arbitrary diameter, situated at the laser aimpoint on the target. A beam which is severely distorted and tilted off-axis will likely result in reduced PIB. Another common metric is peak irradiance at the target, which obviously is diminished as turbulence and thermal blooming effects increase. Finally, we chose to compare the tilt of the far-field spot's centroid from the optical axis, which is another measure of the impact of combined thermal blooming and turbulence effect. In each case, the ideal situation is comparable values for the far-field propagation pattern whether calculated by the HELEEOS – AOTB scaling law model or wave-optics. That said, we remind the reader that we are convolving the outputs from two scaling law models, and as such, one should not expect exact agreement with wave optics.

A comparison of these three metrics, as derived by wave optics and HELEEOS – AOTB, for the four representative scenarios are shown in Tables 3 (PIB) and 4 (peak irradiance and tilt). First, looking at 10 cm PIB (less stringent than 5 cm PIB), the errors are within +/– 25% for all engagements except S2S, where HELEEOS – AOTB is pessimistic by over 30%. Even this error should be considered moderate for a scaling law, but an explanation will be given shortly. Moving to the 5 cm bucket size, errors are small except for the S2S case. Peak irradiance comparisons once again show considerable discrepancy for the S2S engagement, but the HELEEOS – AOTB outcomes are again generally pessimistic, which is desirable for such a model. Finally, looking at centroid tilt, results can be considered to compare quite well with errors always falling in the range of 0% to + 50%.

#188462 - $15.00 USD Received 8 Apr 2013; revised 1 Jun 2013; accepted 3 Jun 2013; published 13 Jun 2013

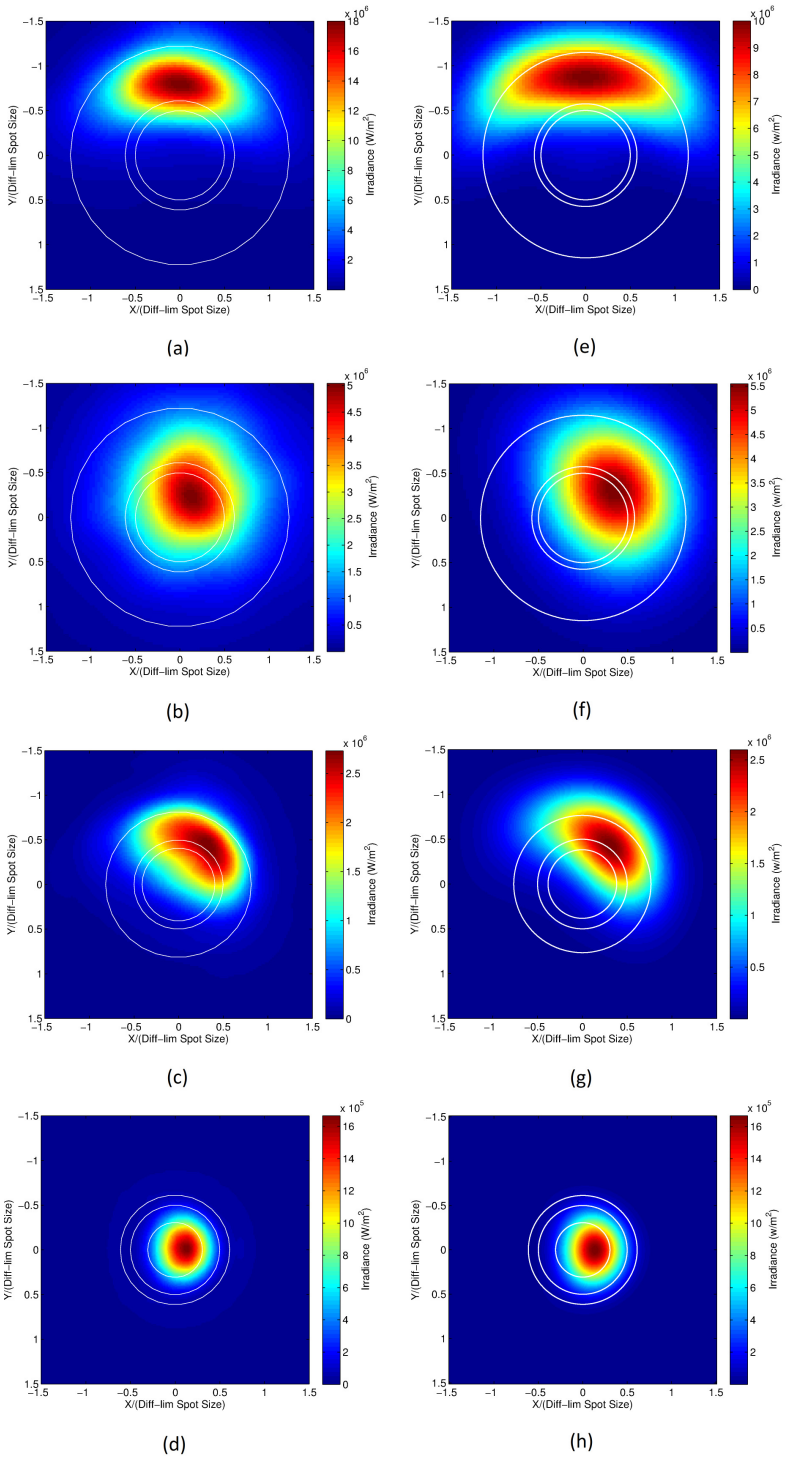

Fig. 5. The irradiance profiles for the wave optics (a-d) and HELEEOS – AOTB (e-h) results with S2S, S2A, A2S, and A2A scenario pairs presented top to bottom, respectively. The general shapes of the spots in each row match well.

#188462 - $15.00 USD Received 8 Apr 2013; revised 1 Jun 2013; accepted 3 Jun 2013; published 13 Jun 2013

Table 3. PIB values from wave optics and HELEEOS – AOTB for 5 and 10 cm diameter buckets and all four scenarios. The error column compares the scaling law to wave optics, which is considered truth.

	5 cm PIB (W)			10 cm PIB* (W)		
	Wave Optics	HELEEOS – AOTB	Error	Wave Optics	HELEEOS – AOTB	Error
S2A	5.89E + 03	6.20E + 03	5.2%	1.28E + 04	1.56E + 04	21.8%
A2S	2.15E + 03	2.08E + 03	–3.3%	7.64E + 03	7.55E + 03	–1.2%
S2S	5.19E + 03	2.50E + 03	–51.9%	2.87E + 04	1.94E + 04	–32.6%
A2A	1.99E + 03	2.10E + 03	5.6%	3.41E + 03	3.95E + 03	15.9%

*This bucket size, often the most relevant in calculation of effect on tactical targets, shows low error.

Table 4. A comparison of peak irradiance and centroid tilt values between wave optics and the proposed scaling law model.

	Peak Irradiance (W/m^2)			Centroid Tilt (rad)		
	Wave Optics	HELEEOS – AOTB	Error	Wave Optics	HELEEOS – AOTB	Error
S2A	4.70E + 06	5.33E + 06	13.4%	2.53E-06	3.60E-06	42.4%
A2S	2.73E + 06	2.71E + 06	–0.6%	2.79E-06	3.07E-06	10.0%
S2S	1.80E + 07	9.47E + 06	–47.4%	5.56E-06	6.63E-06	19.2%
A2A	1.67E + 06	1.62E + 06	–3.3%	7.31E-07	8.74E-07	19.6%

We have noted HELEEOS – AOTB was relatively more pessimistic for S2S PIB calculations. Though this partly may be due to the HELEEOS – AOTB convolution step's inherent inability to fully treat the concurrent interaction of turbulence-induced beam spread and heating effects giving rise to thermal blooming, we also attribute this to the underlying AOTB scaling law, which tends to become more conservative as thermal blooming increases [13]. The S2S scenario experienced the highest levels of blooming because the engagement's propagation path fell outside of the mitigating influence of high levels of aerosol scatter, which dissipates beam irradiance and counters atmospheric heating. The propagation paths associated with the other geometries passed through the high scattering elevated aerosol layer, thus diminishing thermal blooming. Furthermore, the effective cross (clearing) winds were smaller for the S2S scenario as compared to the other scenarios, thus setting conditions for relatively high localized heating and thermal blooming. In fact for the S2S scenario, we found AOTB alone introduced approximately 80% of the peak irradiance error noted in Table 4 and 90% of the 10 cm PIB error shown in Table 3. In summary, the HELEEOS – AOTB model generally errs on the conservative side, which is the preferred error end-state for scaling laws.

4. Conclusion

This paper presented a new HEL scaling law model for fast, enhanced modeling of combined thermal blooming and turbulence effects on high energy laser propagation. The new model utilizes two previously developed scaling laws for DE propagation, one providing the far-field results showing turbulence effects and the other for whole-beam thermal blooming. By convolving the outputs of the two scaling law codes, our results—comparable to those of high-fidelity wave optics simulation both in far-field irradiance displacement and (crescent-shaped) distortion—can be achieved in a small fraction of the time. Such results are of immense utility for HEL evaluations requiring irradiance pattern information either quickly or for large sets of conditions, such as force-on-force engagements or broad-ranging HEL weapon effectiveness research. While the results presented here have been limited to the HELEEOS – AOTB pair, this convolution step should be generally applicable to any pair of scaling law models, with one component specializing in effects distinct from the other. For example, the method could be applied to the High Energy Laser Consolidated Modeling

#188462 - $15.00 USD Received 8 Apr 2013; revised 1 Jun 2013; accepted 3 Jun 2013; published 13 Jun 2013

Engagement Simulation (HELCOMES) – AOTB pair to mesh AOTB's thermal blooming modeling with HELCOMES.

Future research will expand upon HELEEOS – AOTB's capabilities by accounting for the mitigation of thermal blooming by turbulence beam spread and by investigating and incorporating the effect of a random wind component on engagements in which stagnation zones are created along the path. Regarding mitigation of blooming by turbulence, additional AOTB capabilities beyond those demonstrated in this paper may serve toward that end, particularly AOTB's modeling of adaptive optical compensation of thermal blooming in the presence of turbulence. Such an improvement would reduce the method's pessimism in situations when such an effect is significant.

Acknowledgments

The authors recognize the critical support of the High Energy Laser Joint Technology Office in Albuquerque, New Mexico, which sponsored this work. Additionally, we credit Dr. Salvatore Cusumano for the idea of convolving the two scaling laws as a way to capture their integrated effects. Also, we thank the numerous reviewers for their insightful feedback. The views expressed in this paper are those of the authors and do not necessarily reflect the official policy of the U.S. Air Force, the Department of Defense, or U.S. Government.

#188462 - $15.00 USD Received 8 Apr 2013; revised 1 Jun 2013; accepted 3 Jun 2013; published 13 Jun 2013